EDGE ARTICLE

Check for updates

Flavanthrene derivatives as photostable and efficient singlet exciton fission materials†

Xian Fei,‡[a] San Zhang,‡[b] Dong Zhai, [ID] ‡[c] Zhiwei Wang,[b] Jin-Liang Lin,[a] Qi Xiao,[a] Chun-Lin Sun,[a] Weiqiao Deng, [ID] *[c] Chunfeng Zhang,*[b] Wenping Hu*[d] and Hao-Li Zhang [ID] *[ad]

Singlet exciton fission (SF) is believed to have the potential to break the Shockley–Queisser limit for third-generation solar cell devices, so it has attracted great attention. Conventional linear acene based SF materials generally suffer from low triplet energy and poor photostability. We report herein two flavanthrene derivatives, EH-Fla and TIPS-Fla, as new photostable singlet exciton fission materials. These N-doped two-dimensional angular fused acenes have three sets of aromatic Clar sextets, making them significantly more stable than linear acenes with only one sextet. Time-resolved spectroscopy characterization reveals that the SF process occurs in the polycrystalline films of EH-Fla and TIPS-Fla, with maximal triplet yields of 32% and 159%, respectively. The SF processes of these two molecules are mediated by excimer states. In EH-Fla, the low-lying excimer prevents the SF process from occurring effectively, resulting in a low triplet yield. In contrast, the excimer state in TIPS-Fla is mixed with strong CT coupling, which prompts efficient SF and results in a high triplet yield. Our results show that flavanthrene is a promising SF chromophore for photoenergy conversion applications, while a fine-tune of the intermolecular interaction is crucial for achieving high SF efficiency.

Introduction

Singlet exciton fission (SF) is a spin-allowed multi-exciton generation process, in which one high-energy singlet exciton is transformed into two or more low-energy triplet excitons.[1–3] SF was first discovered in anthracene crystals in 1965,[4] but the interest in SF did not renew until its application potential in photon energy conversion was unveiled in the recent decade. With multi-exciton generation capability, SF is believed to have the potential to break the 33% Shockley–Queisser limit by overcoming thermalization losses in third-generation solar cell devices.[5–8] However, the practical applications of SF materials

are greatly hindered by the limited availability of suitable materials.[9–12] Extensive efforts have been made to develop highly efficient SF materials and to understand their photodynamic properties.

The basic energetic requirement for SF to occur is that the singlet exciton energy (S_1) is greater than or approximately equal to twice the triplet exciton energy (T_1).[1,2] Importantly, intermolecular interaction between neighbouring chromophores in a solid-state plays a crucial role, as SF relies on appropriate electronic coupling for fast and effective energy and spin exchange to take place.[1,13] Previous investigations into typical SF chromophores, such as pentacene, tetracene, perylenediimide, terrylenediimide, and diketopyrrolopyrrole, have revealed that the SF behaviours are strongly dependent on their molecular packing.[14–19] Therefore, clarifying the influence of intermolecular packing on the SF process in molecular aggregates and understanding the correlation between intermolecular packing and photodynamic behaviours is critical for realizing effective SF materials.

For practical applications, an ideal SF material also needs to meet several other criteria, including high SF yield, high triplet energy, strong light absorption capacity and excellent photostability.[8] To date, the most widely studied candidates for SF are still acenes and their derivatives, because of their high triplet yield and well-studied triplet behaviours.[20–23] However, linear acenes, such as pentacene, generally suffer from low triplet exciton energy (0.86 eV) and poor photostability. Developing

[a]State Key Laboratory of Applied Organic Chemistry, College of Chemistry and Chemical Engineering, Lanzhou University, Lanzhou, 730000, China. E-mail: haoli.zhang@lzu.edu.cn

[b]National Laboratory of Solid State Microstructures, Collaborative Innovation Centre of Advanced Microstructures, School of Physics, Nanjing University, Nanjing, 210093, China. E-mail: cfzhang@nju.edu.cn

[c]Institute of Molecular Sciences and Engineering, Institute of Frontier and Interdisciplinary Science, Shandong University, Qingdao, 266237, China. E-mail: dengwq@sdu.edu.cn

[d]Tianjin Key Laboratory of Molecular Optoelectronic Sciences, School of Science, Institute of Molecular Aggregation Science, Tianjin University, 300072, Tianjin, China. E-mail: huwp@tju.edu.cn

‡ These authors contributed equally to this work.

new photo-stable SF materials with appropriate triplet exciton energy is of great importance for the design of ideal SF materials. One of the common strategies for improving the photostability of acenes is to lower the frontier molecular orbitals by introducing electron-withdrawing groups, such as diimide groups.[24,25] Besides, we have demonstrated that hetero atoms containing pentacenes are more stable than pentacenes, and their SF properties can be adjusted by changing the position and number of the nitrogen atom.[26–28] The low triplet energies of the acenes can be attributed to their migratory Clar's sextets resulting in large localized diradical character, which compromises chemical stability.[29] Therefore, increasing the number of Clar's sextets could be an efficient way to obtain stable SF materials, as more Clar's sextets can reduce the diradical character of the acenes and modulate their triplet energy.[30–33]

Herein, we report the design of photostable SF materials based on the flavanthrene structure, which has an N-doped two-dimensional angular fused acene framework. Compared with linear acenes, two-dimensional angular fused acenes have more aromatic Clar's sextets, making them significantly more stable than linear acenes with only one sextet.[34,35] Meanwhile, N-doping can raise the ionization potential of the system, making the molecular less susceptible to oxidization.[26,28] When the number of benzene rings is the same, the bandgap of the angular fused structure is higher, thereby raising the energy of the singlet exciton.[34] Meanwhile, when nitrogen atoms are introduced, the molecular energy levels can be adjusted by the number and position of nitrogen atoms.[28,31,36] Within the scope of our knowledge, there has been no report of two-dimensional angular fused acenes with SF properties to date. We demonstrate that two soluble flavanthrene derivatives exhibit strong photoabsorption and excellent photostability. Photodynamic investigation of their exciton behaviours reveals a strong dependence of SF efficiency on their intermolecular interactions in their crystals.

Results and discussion

Herein, we synthesized two soluble flavanthrenes, EH-Fla and TIPS-Fla, which have 2-ethylhexyloxy and triisopropylsilylacetylene (TIPS) units as the soluble side groups (Fig. 1). The calculations, based on density functional theory (DFT) and time-dependent dense functional theory (TD-DFT), indicate that the triplet exciton energies (T_1) are 1.38 eV (EH-Fla) and 1.15 eV (TIPS-Fla), and the singlet exciton energies (S_1) are 2.48 eV (Fla-EH) and 2.3 eV (TIPS-Fla). From the calculations, the S_1 energies of both molecules are approximately equal to twice their T_1, which meets the energetic requirements for SF to take place.

The single-crystal structure of EH-Fla was grown in chloroform by slow solvent evaporation. The crystal form is monoclinic in the $P2_1/c$ space group, in which EH-Fla has a slip-stacked dimeric structure with a 3.31 Å π–π distance. The single crystal of TIPS-Fla has been reported in our previous research,[37] which is in the $C2/c$ space group with a 3.38 Å π–π distance. The molecular scaffold of TIPS-Fla is nearly a plane, only slightly distorted due to the steric interaction between the TIPS groups

Fig. 1 Chemical structure of EH-Fla (a) and TIPS-Fla (b), and the red circle represents Clar's sextets. Crystal structures of EH-Fla (c) and TIPS-Fla (d). EH-Fla dimer (e) and TIPS-Fla dimer (f) extracted from the crystal structures.

and neighbouring flavanthrene cores. The molecules in the dimer are asymmetrically staggered due to the large steric hindrance of TIPS units.

EH-Fla can be spin cast into thin films due to its good solubility. We cast the EH-Fla thin films on quartz and then annealed them at 100 °C for 30 min to improve crystallinity. The TIPS-Fla films were deposited on quartz using a home-made vacuum-tube furnace. The natural aggregation in the films was characterized by grazing-incidence wide-angle X-ray scattering (GIWAXS). The in-plane and out-of plane line cuts from GIWAXS were compared with the simulated powder patterns, as shown in Fig. S1.† The diffractograms obtained by GIWAXS resemble the simulated powder pattern, which implies that the intermolecular interactions observed in the thin film are similar to those in the single-crystal structure.

The ultimate goal of exploiting SF-capable materials is to access triplet states without sacrificing chemical stability. The ambient stability of flavanthrene was compared with that of TIPS-tetracene and TIPS-pentacene. From Fig. S2,† we can see that both TIPS-tetracene and TIPS-pentacene almost decomposed completely after about 8 hours under 18 W UV lamp irradiation. In contrast, after 80 hours of UV irradiation, the absorption of EH-Fla and TIPS-Fla solutions remained at 92% and 99%, respectively. Meanwhile, EH-Fla and TIPS-Fla also exhibited excellent stability in films and their absorption remained above 95% after 80 hours of UV irradiation (Fig. S3†).

Fig. 2 shows the absorption spectra of EH-Fla and TIPS-Fla in dichloromethane solution. Compared to EH-Fla, the absorption of TIPS-Fla is bathochromic shifted by approximately 35 nm, which is attributed to that the TIPS groups expand the π-conjugation of the flavanthrene skeleton *via* the triple bonds. The S_1 of EH-Fla and TIPS-Fla in solution is 2.4 eV and 2.24 eV respectively, which is estimated from the absorption and emission spectra in dichloromethane solutions. Rao *et al.* indicated that strong absorption is needed for the application of SF sensitized solar cells to reduce device thickness and mitigate

Fig. 2 Steady-state absorption (solid lines) and emission spectra (dashed lines) of dilute solutions (blue) and polycrystalline films (green) of EH-Fla (a) and TIPS-Fla (b).

problems with triplet diffusion.[8] Both EH-Fla and TIPS-Fla show strong absorption in the visible region and the molar extinction coefficient of TIPS-Fla reaches almost 10^5 M^{-1} cm^{-1} (Fig. S4†), higher than most reported SF materials.

Phosphorescence spectra of EH-Fla and TIPS-Fla in solution are almost the same (Fig. S5†), suggesting that the side chains have little effect on the triplet energy. The T_1 energies of EH-Fla and TIPS-Fla are both estimated to be around 1.08 eV from their phosphorescence spectra, slightly lower than that predicted using TD-DFT calculations. The measured S_1 is approximately equal to twice the T_1 in solution, confirming that both EH-Fla and TIPS-Fla meet the energetic conditions for SF.

It is known that the intermolecular interactions, particularly long-range Coulomb coupling and short-range charge-transfer (CT) between chromophores, play important roles in their exciton behaviours.[38] Based on a simplified Kasha's model, long-range Coulomb coupling induced packing mode between chromophores is usually described as J- and H-aggregates.[39] Kasha originally defined two kinds of aggregation through the relative orientation of transition dipole moments (θ). The "head-to-tail" orientations ($\theta \approx 0$) give rise to J-aggregates, while "side-by-side" orientations ($\theta \approx \pi/2$) lead to H-aggregates. H-aggregates are characterized by a spectral blue-shift with diminished ratios of the first and second vibronic transitions (A_{0-0}/A_{0-1}) relative to the monomers, while the J-aggregate shows a spectral redshift with an increased A_{0-0}/A_{0-1} ratio.[38,39]

The θ value of EH-Fla is calculated to be 42° based on its crystal structure, which is roughly in the middle range between 0° and 90°, so it is expected that it may exhibit both J and H characteristics. The absorption spectra of EH-Fla in solutions and thin films are compared in Fig. 2. In solution, the 0–0 transition of EH-Fla is found at 514 nm as the strongest absorption peak. In the thin film, the 0–0 transition is barely observed at 536 nm as a shoulder. The 22 nm red-shift from the monomer state to the aggregated state suggests a J-aggregation characteristic. Meanwhile, the A_{0-0}/A_{0-1} ratio of EH-Fla in solutions is around 2.47, which is drastically decreased to 0.6 in the thin film, showing a significant H-aggregation characteristic.

The θ value for TIPS-Fla is 68°, higher than that for EH-Fla. From the θ values, one may expect stronger H-aggregation characteristics of TIPS-Fla than EH-Fla, but the absorption spectra suggest strong J-aggregation characteristics of TIPS-Fla. First, TIPS-Fla shows a strong 0–0 absorption peak in the thin film, which has the highest absorbance in the whole spectral

range. The 0–0 transition in the film is bathochromic for 44 nm compared to its solution spectrum. Both strong absorption and the significant red-shift of the 0–0 absorption are consistent with J-aggregation characteristics. Meanwhile, the A_{0-0}/A_{0-1} of the TIPS-Fla film is 1.06, which is also reduced compared to the monomer A_{0-0}/A_{0-1} in solution (2.47), showing a weak H-aggregation characteristic. As discussed above, Fig. 2 indicates that TIPS-Fla exhibits much stronger J characteristics in the thin film than EH-Fla, which indicates that other strong intermolecular interactions besides Coulomb coupling are playing a dominating role in the crystal of TIPS-Fla.

From the crystal structures, the inter-plane distances of both molecules are about 3.3 Å, indicating strong π–π interaction. This tight arrangement induces significant orbital overlap with neighbouring molecules, resulting in non-negligible CT coupling.[14] The calculation method for the CT coupling is shown in the Theoretical calculation section of the ESI.† The CT coupling of EH-Fla and TIPS-Fla is -1435 cm^{-1} and -5153 cm^{-1}, respectively, which indicates that the CT coupling effect in TIPS-Fla is dramatically stronger than that in EH-Fla. Previous studies have pointed out that a negative CT coupling will lead to a red-shifted absorption peak and an increase in the A_{0-0}/A_{0-1} ratio.[38,39] It is reasonable to attribute the apparently stronger J characteristics of TIPS-Fla observed in the absorption spectra to its significantly more negative CT coupling than that of EH-Fla.

Compared to the fluorescence in solution, the thin film fluorescence of EH-Fla and TIPS-Fla is significantly red-shifted and featureless, which indicates the existence of an excimer. The fluorescence quantum yields of EH-Fla and TIPS-Fla in solution are 64% and 82%, respectively. The fluorescence quantum yield of EH-Fla film is very low ($\sim$0.1%), and the fluorescence lifetime is 1.36 ns. The TIPS-Fla film shows a higher fluorescence quantum yield (2.06%) than EH-Fla, and the fluorescence lifetimes are 0.4 ns (89%) and 2.66 ns (11%) from a bi-exponential fit. The fluorescence quantum yields of the two samples in the films are significantly lower than those in the solutions, indicating that there are other decay pathways in the films.

The different electronic coupling properties of EH-Fla and TIPS-Fla are expected to have a strong impact on their photophysical behaviours. We then investigated the excited state dynamics of the two compounds in both solution and solid states through femtosecond transient absorption spectroscopy (fs-TA). First, the fs-TA spectra of EH-Fla and TIPS-Fla in dilute dichloromethane solutions is shown in Fig. S6.† The singlet exciton lifetimes of EH-Fla and TIPS-Fla are 3.34 ns and 1.93 ns respectively. No evidence of long-lived species is in their solutions, indicating that triplet formation associated with intersystem crossing is neglectable.

The fs-TA spectra of EH-Fla and TIPS-Fla thin films were acquired by exciting the samples at 400 nm with an excitation energy of about 0.2 μJ. Fig. 3 shows the dynamic curve at different wavelengths and evolution-associated spectra (EAS) of both films. The fs-TA spectrum of EH-Fla (Fig. 3a) at early times exhibits ground-state bleaching (GSB) from 450 to 550 nm, which is consistent with the steady-state absorption (Fig. 2). The

Fig. 3 (a–c) fs-TA spectra at different delay times, the dynamic curve at different wavelengths and the evolution-associated spectra obtained through global fitting of EH-Fla. (d–f) fs-TA spectra at different delay times, the dynamic curve at different wavelengths and the evolution-associated spectra obtained through global fitting of TIPS-Fla.

excited-state absorption (ESA) features from 580 to 750 nm, which are broadened compared to those in solution (Fig. S6a†). At later times, a new ESA appears at 520–540 nm overlapping with GSB, indicating that a new species was generated. The fs-TA spectrum of TIPS-Fla (Fig. 3d) shows GSB from 450 nm to 650 nm and ESA at 650–750 nm at the beginning. At later times, a new spectral feature emerged at 540 nm overlapping with GSB.

The evolution-associated spectra (Fig. 3c and f) were obtained from the Glotaran program.[40] The fs-TA spectrum of EH-Fla is best fitted to a three-species sequential A → B → C → GS model (details shown in the ESI†). For EH-Fla (Fig. 3c), the initial state A shows a broad, featureless ESA signal. The near-infrared fs-TA is shown in Fig. S9.† The ESA signal of EH-Fla between 850 nm and 950 nm is part of the broad peak in the visible region. It is known that transient absorption spectra of aromatic excimers typically present as broadened, featureless absorptions in the visible region.[17,41–43] Therefore, state A indicates excimer state formation within 200 fs. Previous discussions of aromatic excimers have identified a two-step mechanism, which suggests that a relaxed excimer state is generated from a non-relaxed or hot excimer state.[44,45] State B forms in $\tau_{A \to B} = 26.5$ ps and shows an increasing ESA signal, which is assigned as a structural relaxation process to form a relaxed excimer geometry.[43] State B then decays to form state C in $\tau_{B \to C} = 463$ ps. State C is assigned to a triplet pair which is discussed below and in the ESI (Fig. S13 and S14†). The nanosecond transient absorption (ns-TA) spectra of EH-Fla are presented in Fig. S14,† which gives the lifetime of state C as 176.3 ns with a single-exponential decay.

The fs-TA spectrum of TIPS-Fla is best fitted using a two species sequential A → B → GS model (details shown in the ESI†). For TIPS-Fla (Fig. 3f), state A shows a broad and featureless ESA signal above 650 nm, which extends to around 1000 nm (Fig. S9†), suggesting the presence of an excimer feature in state A. State B evolves from an excimer in $\tau_{A \to B} = 500$ ps, which is assigned to a triplet pair. The ns-TA spectra (Fig. S14b and d†) indicate that the lifetime of state C is around 190.5 ns with a single-exponential decay.

The triplet nature of state C of EH-Fla and state B of TIPS-Fla is confirmed by a triplet sensitization experiment. Fig. S17a† shows that the spectrum of the triplet obtained from sensitization of EH-Fla matches well with the state C and ns-TA spectra at 50 ns, indicating that the state C is a triplet exciton. In the TIPS-Fla film, the spectra of the triplet from sensitization, state B and ns-TA spectra at 98 ns show very similar spectral features, confirming that the state B of TIPS-Fla is also a triplet exciton (Fig. S17b†). Further analysis of the decay dynamics at different temperatures reveals that the state C of EH-Fla and state B of TIPS-Fla are triplet pairs (details shown in ESI Fig. S13 and S14†).

The triplet yields are calculated by the energy transfer method, in which a suitable triplet sensitizer undergoes energy transfer to the triplet state of the SF chromophore (details shown in the ESI†).[20] To evaluate possible thermal effects on the transient spectra, we have measured the ns-TA spectra of thin-film samples on sapphire and quartz substrates. The kinetic decay curves obtained on different substrates show that the kinetic process is not significantly different after 10 ns (Fig. S18†), suggesting that the thermal effect on transient spectra can be excluded. The triplet yields of TIPS-Fla and EH-Fla are then calculated to be 159% and 32% at 4 ns, respectively.

As shown in the above spectra, excimers are observed in the films of both compounds. Several previous studies have explored excimer-mediated SF processes in concentrated pentacene solutions, perylenediimide dimers, and films of diketopyrrolopyrrole, terrylenediimide, and dipyrrolonaphthyridinedione.[18,28,45,46] In the excimer-mediated process, SF occurs in two steps. First, a fast transition from the $^1(S_1S_0)$ state to the excimer intermediate. Second, a slower transition from the excimer intermediate to $^1(T_1T_1)$ occurs using the CT state in a superexchange interaction.[47] An excimer state can be defined as a linear combination of Frenkel exciton and CT states.[48,49] An excimer with a significant CT state contribution could drive the excimer to SF via enhancing electronic coupling between the singlet state and triplet pair states.[45,48,50] In this work, the CT coupling of EH-Fla and TIPS-Fla is calculated to be -1435 cm^{-1} and -5153 cm^{-1}, respectively.

Table 1 The energy of the singlet exciton ($E(S_1)$), triplet exciton ($E(T_1)$), excimer ($E(Ex)$) and charge-transfer state ($E(CT)$)

	$E(S_1)^a$/eV	$E(T_1)^b$/eV	$E(Ex)^a$/eV	$E(CT)^c$/eV
EH-Fla	2.25	1.08	2.11	2.57
TIPS-Fla	2.06	1.08	2.0	2.18

^{a} Values obtained from the experiment on films. ^{b} Values obtained from the experiment on solution. ^{c} Values obtained from theoretical calculations.
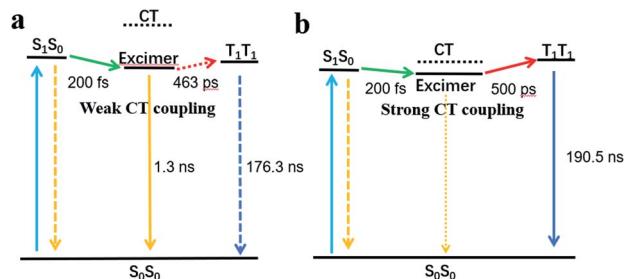

Fig. 4 Jablonski-type diagram of the main kinetic model for EH-Fla (a) and TIPS-Fla (b) in thin films. In the EH-Fla film, the excimer acts as a trap, which competes with the SF process. SF in the TIPS-Fla film occurs through an excimer-mediated mechanism with strong CT coupling and a close CT energy.

The result indicates that the CT coupling effect in TIPS-Fla is significantly stronger than that in EH-Fla, which is more favorable to drive the excited-state population escaping from the excimer trap and promote an efficient SF process.

Meanwhile, excimer formation changes the free energy landscape for SF, which is expected to lower the S_1 and CT energy.[49] When the excimer, S_1 and CT states are close in energy, it is favorable for the mixing of these states to promote SF.[46,47,49] The calculated results show that the CT state energies of EH-Fla are 2.57 eV and 0.46 eV above the excimer (2.11 eV) (Table 1). Such a high CT state of EH-Fla is unfavorable for SF to occur *via* a superexchange interaction. Consequently, the low-lying excimer state of EH-Fla acts as a trap state and inhibits SF, resulting in a low triplet yield. In contrast, TIPS-Fla has a strong CT state at 2.18 eV, which is very close to both the singlet (2.06 eV) and excimer (2.0 eV) states and therefore is favorable for SF to occur (Fig. 4).

Conclusion

In conclusion, we report a new molecular design strategy for efficient and photostable SF materials, which is based on the N-doped two-dimensional angular fused acene framework of flavanthrene. Both EH-Fla and TIPS-Fla exhibit a triplet exciton energy of 1.08 eV, strong light absorption capacity and superior photostability. Meanwhile, intermolecular interactions strongly affect the SF efficiency of the two derivatives. In the films of EH-Fla, both weak CT coupling and high CT energy inhibit the efficient occurrence of SF, resulting in a low triplet yield (32%). In contrast, the strong CT coupling along with the suitable CT energy of TIPS-Fla can efficiently drive the excited-state population escaping from the excimer trap and promote a SF process, resulting in a high triplet yield (159%). Further improvement of the SF yield may be achieved by optimizing molecular packing by fine tuning the structure of the side groups and enhancing CT coupling. TIPS-Fla exhibits several attractive features, including high SF efficiency, a high blue-green light absorption coefficient, high triplet energy and high photostability. The results of this study indicate that flavanthrene-based chromophore is promising for SF-based photo energy conversion applications.

Data availability

All experimental and computational data is available in the ESI.†

Author contributions

H.-L. Zhang, W. P. Hu, C. F. Zhang and W. Q. Deng came up with the idea and elaborated the manuscript. X. Fei conducted the sample preparation, physical characterization and wrote the first draft of the manuscript. Z. W. Wang and S. Zhang performed the ultrafast spectroscopy test; D. Zhai performed the DFT calculations. J.-L. Lin contributed to the synthesis experiment. Q. Xiao contributed to the test of film thickness. C.-L. Sun provided critical advice during the manuscript writing.

Conflicts of interest

There are no conflicts to declare.

Acknowledgements

Notes and references

1 M. B. S. J. Michl, *Chem. Rev.*, 2010, **110**, 6891–6936.
2 M. B. Smith and J. Michl, *Annu. Rev. Phys. Chem.*, 2013, **64**, 361–386.
3 D. Casanova, *Chem. Rev.*, 2018, **118**, 7164–7207.
4 S. Singh, W. J. Jones, W. Siebrand, B. P. Stoicheff and W. G. Schneider, *J. Chem. Phys.*, 1965, **42**, 330–342.
5 I. Paci, J. C. Johnson, X. Chen, G. Rana, D. Popovic, D. E. David, A. J. Nozik, M. A. Ratner and J. Michl, *J. Am. Chem. Soc.*, 2006, **128**, 16546–16553.
6 J. Lee, P. Jadhav, P. D. Reusswig, S. R. Yost, N. J. Thompson, D. N. Congreve, E. Hontz, T. Van Voorhis and M. A. Baldo, *Acc. Chem. Res.*, 2013, **46**, 1300–1311.

7 J. Xia, S. N. Sanders, W. Cheng, J. Z. Low, J. Liu, L. M. Campos and T. Sun, *Adv. Mater.*, 2017, **29**, 1601652.

8 A. Rao and R. H. Friend, *Nat. Rev. Mater.*, 2017, **2**, 17063.

9 D. N. Congreve, J. Lee, N. J. Thompson, E. Hontz, S. R. Yost, P. D. Reusswig, M. E. Bahlke, S. Reineke, T. Van Voorhis and M. A. Baldo, *Science*, 2013, **340**, 334–337.

10 A. Kunzmann, M. Gruber, R. Casillas, J. Zirzlmeier, M. Stanzel, W. Peukert, R. R. Tykwinski and D. M. Guldi, *Angew. Chem., Int. Ed. Engl.*, 2018, **57**, 10742–10747.

11 M. Einzinger, T. Wu, J. F. Kompalla, H. L. Smith, C. F. Perkinson, L. Nienhaus, S. Wieghold, D. N. Congreve, A. Kahn, M. G. Bawendi and M. A. Baldo, *Nature*, 2019, **571**, 90–94.

12 L. M. Pazos-Outon, J. M. Lee, M. H. Futscher, A. Kirch, M. Tabachnyk, R. H. Friend and B. Ehrler, *ACS Energy Lett.*, 2017, **2**, 476–480.

13 J. C. Johnson, A. J. Nozik and J. Michl, *Acc. Chem. Res.*, 2013, **46**, 1290–1299.

14 A. K. Le, J. A. Bender, D. H. Arias, D. E. Cotton, J. C. Johnson and S. T. Roberts, *J. Am. Chem. Soc.*, 2018, **140**, 814–826.

15 S. W. Eaton, L. E. Shoer, S. D. Karlen, S. M. Dyar, E. A. Margulies, B. S. Veldkamp, C. Ramanan, D. A. Hartzler, S. Savikhin, T. J. Marks and M. R. Wasielewski, *J. Am. Chem. Soc.*, 2013, **135**, 14701–14712.

16 S. Masoomi-Godarzi, C. R. Hall, B. Zhang, M. A. Gregory, J. M. White, W. W. H. Wong, K. P. Ghiggino, T. A. Smith and D. J. Jones, *J. Phys. Chem. C*, 2020, **124**, 11574–11585.

17 E. A. Margulies, J. L. Logsdon, C. E. Miller, L. Ma, E. Simonoff, R. M. Young, G. C. Schatz and M. R. Wasielewski, *J. Am. Chem. Soc.*, 2017, **139**, 663–671.

18 C. M. Mauck, P. E. Hartnett, E. A. Margulies, L. Ma, C. E. Miller, G. C. Schatz, T. J. Marks and M. R. Wasielewski, *J. Am. Chem. Soc.*, 2016, **138**, 11749–11761.

19 C. Sutton, N. R. Tummala, D. Beljonne and J.-L. Brédas, *Chem. Mater.*, 2017, **29**, 2777–2787.

20 B. J. Walker, A. J. Musser, D. Beljonne and R. H. Friend, *Nat. Chem.*, 2013, **5**, 1019–1024.

21 A. J. Musser, M. Liebel, C. Schnedermann, T. Wende, T. B. Kehoe, A. Rao and P. Kukura, *Nat. Phys.*, 2015, **11**, 352–357.

22 N. V. Korovina, S. Das, Z. Nett, X. Feng, J. Joy, R. Haiges, A. I. Krylov, S. E. Bradforth and M. E. Thompson, *J. Am. Chem. Soc.*, 2016, **138**, 617–627.

23 S. N. Sanders, E. Kumarasamy, A. B. Pun, M. T. Trinh, B. Choi, J. Xia, E. J. Taffet, J. Z. Low, J. R. Miller, X. Roy, X. Y. Zhu, M. L. Steigerwald, M. Y. Sfeir and L. M. Campos, *J. Am. Chem. Soc.*, 2015, **137**, 8965–8972.

24 S. Katsuta, K. Tanaka, Y. Maruya, S. Mori, S. Masuo, T. Okujima, H. Uno, K.-i. Nakayama and H. Yamada, *Chem. Commun.*, 2011, **47**, 10112–10114.

25 X. Cui, C. Xiao, T. Winands, T. Koch, Y. Li, L. Zhang, N. L. Doltsinis and Z. Wang, *J. Am. Chem. Soc.*, 2018, **140**, 12175–12180.

26 Y.-Y. Liu, C.-L. Song, W.-J. Zeng, K.-G. Zhou, Z.-F. Shi, C.-B. Ma, F. Yang, H.-L. Zhang and X. Gong, *J. Am. Chem. Soc.*, 2010, **132**, 16349–16351.

27 A. L. Appleton, S. M. Brombosz, S. Barlow, J. S. Sears, J.-L. Bredas, S. R. Marder and U. H. F. Bunz, *Nat. Commun.*, 2010, **1**, 91.

28 Y. D. Zhang, Y. Wu, Y. Xu, Q. Wang, K. Liu, J. W. Chen, J. J. Cao, C. Zhang, H. Fu and H. L. Zhang, *J. Am. Chem. Soc.*, 2016, **138**, 6739–6745.

29 K. J. Fallon, P. Budden, E. Salvadori, A. M. Ganose, C. N. Savory, L. Eyre, S. Dowland, Q. Ai, S. Goodlett, C. Risko, D. O. Scanlon, C. W. M. Kay, A. Rao, R. H. Friend, A. J. Musser and H. Bronstein, *J. Am. Chem. Soc.*, 2019, **141**, 13867–13876.

30 S. Lukman, J. M. Richter, L. Yang, P. Hu, J. Wu, N. C. Greenham and A. J. Musser, *J. Am. Chem. Soc.*, 2017, **139**, 18376–18385.

31 J. P. Mora-Fuentes, I. Papadopoulos, D. Thiel, R. Alvarez-Boto, D. Cortizo-Lacalle, T. Clark, M. Melle-Franco, D. M. Guldi and A. Mateo-Alonso, *Angew. Chem., Int. Ed. Engl.*, 2020, **59**, 1113–1117.

32 P. J. Budden, L. R. Weiss, M. Muller, N. A. Panjwani, S. Dowland, J. R. Allardice, M. Ganschow, J. Freudenberg, J. Behrends, U. H. F. Bunz and R. H. Friend, *Nat. Commun.*, 2021, **12**, 1527.

33 Y. Jue Bae, M. D. Krzyaniak, M. B. Majewski, M. Desroches, J. F. Morin, Y. L. Wu and M. R. Wasielewski, *Chempluschem*, 2019, **84**, 1432–1438.

34 L. Zhang, Y. Cao, N. S. Colella, Y. Liang, J. L. Bredas, K. N. Houk and A. L. Briseno, *Acc. Chem. Res.*, 2015, **48**, 500–509.

35 L. Zhang, A. Fonari, Y. Liu, A. L. Hoyt, H. Lee, D. Granger, S. Parkin, T. P. Russell, J. E. Anthony, J. L. Bredas, V. Coropceanu and A. L. Briseno, *J. Am. Chem. Soc.*, 2014, **136**, 9248–9251.

36 N. Wollscheid, B. Günther, V. J. Rao, F. J. Berger, J. L. P. Lustres, M. Motzkus, J. Zaumseil, L. H. Gade, S. Höfener and T. Buckup, *J. Phys. Chem. A*, 2020, **124**, 7857–7868.

37 L. Zhang, A. Fonari, Y. Zhang, G. Zhao, V. Coropceanu, W. Hu, S. Parkin, J. L. Bredas and A. L. Briseno, *Chem.–Eur. J.*, 2013, **19**, 17907–17916.

38 N. J. Hestand and F. C. Spano, *Chem. Rev.*, 2018, **118**, 7069–7163.

39 N. J. Hestand and F. C. Spano, *Acc. Chem. Res.*, 2017, **50**, 341–350.

40 J. J. Snellenburg, S. P. Laptenok, R. Seger, K. M. Mullen and I. H. M. van Stokkum, *J. Stat. Softw.*, 2012, **49**, 1–22.

41 R. M. Young and M. R. Wasielewski, *Acc. Chem. Res.*, 2020, **53**, 1957–1968.

42 E. A. Margulies, C. E. Miller, Y. Wu, L. Ma, G. C. Schatz, R. M. Young and M. R. Wasielewski, *Nat. Chem.*, 2016, **8**, 1120–1125.

43 Y. Hong, J. Kim, W. Kim, C. Kaufmann, H. Kim, F. Wurthner and D. Kim, *J. Am. Chem. Soc.*, 2020, **142**, 7845–7857.

44 L. Ma, K. J. Tan, H. Jiang, C. Kloc, M. E. Michel-Beyerle and G. G. Gurzadyan, *J. Phys. Chem. A*, 2014, **118**, 838–843.

45 Y. Hong, J. Kim, W. Kim, C. Kaufmann, H. Kim, F. Wurthner and D. Kim, *J. Am. Chem. Soc.*, 2020, **142**, 7845–7857.

46 L. Wang, W. Cai, J. Sun, Y. Wu, B. Zhang, X. Tian, S. Guo, W. Liang, H. Fu and J. Yao, *J. Phys. Chem. Lett.*, 2021, **12**, 12276–12282.

47 C. E. Miller, M. R. Wasielewski and G. C. Schatz, *J. Phys. Chem. C*, 2017, **121**, 10345–10350.

48 Y. J. Bae, D. Shimizu, J. D. Schultz, G. Kang, J. Zhou, G. C. Schatz, A. Osuka and M. R. Wasielewski, *J. Phys. Chem. A*, 2020, **124**, 8478–8487.

49 K. Miyata, F. S. Conrad-Burton, F. L. Geyer and X. Y. Zhu, *Chem. Rev.*, 2019, **119**, 4261–4292.

50 R. M. Young and M. R. Wasielewski, *Acc. Chem. Res.*, 2020, **53**, 1957–1968.